Chapter 7

The Mechanisms for the Oxidative Addition of Imidazolium Salts to a Group 9 Transition Metal Atom (Co^0, Rh^0, and Ir^0) and a Group 10 Transition Metal Atom (Ni^0, Pd^0, and Pt^0): A Theoretical Study

Hsin-Yi Liao, Jia-Syun Lu and Ming-Der Su

Additional information is available at the end of the chapter

http://dx.doi.org/10.5772/67567

Abstract

The potential energy surfaces of the oxidative addition reactions, L_2M + imidazolium cation → product and CpM′L + imidazolium cation → product (M = Ni, Pd, Pt; M′ = Co, Rh, Ir; Cp = η^5-C_5H_5; L = 1,3-aryl-N-heterocyclic carbene (NHC), aryl = 2,4,6-trimethylphenyl), are studied at the M06-L/Def2-SVP level of theory. The theoretical findings show that the singlet-triplet splitting ($\Delta E_{st} = E_{triplet} - E_{singlet}$) for the L_2M and CpM′L species can be used to predict the reactivity for their oxidative additions. That is to say, current theoretical evidence suggests that both a 14-electron L_2M complex and a 16-electron CpM′Lcomplex with a better electron-donating ligand L (such as NHC) result in a reduced ΔE_{st} value and facilitate the oxidative addition to the saturated C—H bond. The theoretical results for this study are in good agreement with the obtainable experimental results and allow a number of predictions to be made.

Keywords: oxidative addition reactions, group 9 elements, group 10 elements, imidazolium and density functional theory

1. Introduction

Recent studies involving the chemistry of the heterocyclic nitrogen carbene complexes of transition metals have demonstrated that they can act as precatalysts for a variety of reactions [1–11]. These new species offer many opportunities to advance this field of study [12–30]. The use of palladium carbene complexes for the Heck reaction [31–34] and platinum carbene compounds for the C—H activation reactions [11] has created new opportunities in catalytic chemistry.

Over the last two decades, imidazolium-based ionic liquids have also found many applications in catalysis [35–39], or as nonaqueous alternatives for biphasic catalysis [4, 40–42]. The studies by Cavell and co-workers [43] showed that the reaction of imidazolium-based ionic liquids with low-valence Ni^0 and σ-donor ligands that bear Pd^0 is an easy procedure for the production of unusually stable carbene-metal-hydride complexes (see **Scheme 1**). The major feature of the study was the direct formation of a carbene-metal-hydride, which offers an atom-efficient direct route to an active catalytic species. Besides these experimental facts, it is not surprising that N-heterocyclic carbenes (NHCs) [44–46] have found applications in a series of catalytic reactions, such as amination reactions, the Suzuki-Miyaura and Sonogashira coupling reactions, hydroformylation, hydrosilylation, and polymerization and olefin metathesis [47–50].

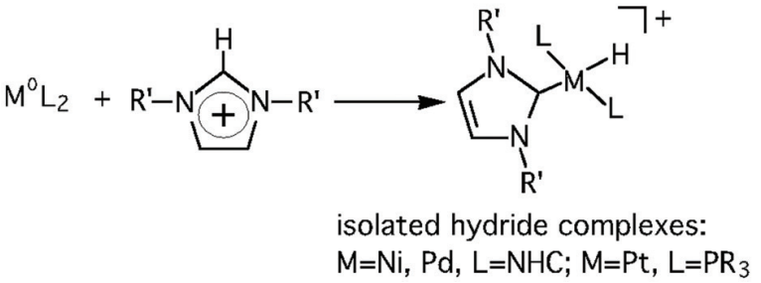

Scheme 1.

The crucial experimental works that are presented in **Scheme 1** inspire this study of the potential energy surfaces of these oxidative addition reactions, using density functional theory (DFT). There have been a number of reports concerning the conventional oxidative additions-reductive eliminations of alkanes to low-valence metals, which has led to an understanding of the factors that affect these reactions [51–56]. These studies have mostly focused on the catalytic reactions of saturated hydrocarbons to zerovalent group 10 elements (i.e., Ni, Pd, and Pt). To the authors' best knowledge, there has been neither experimental nor theoretical study of the catalytic oxidative addition reactions for the group 9 atoms (i.e., Co, Rh, and Ir) or the imidazolium cation. This study gives a thorough understanding of the catalytic reactions for potential transition metal complexes with imidazolium cations (ICs). Accordingly, a study of the important C—H activation reactions, Eqs. (1) and (2), is undertaken:

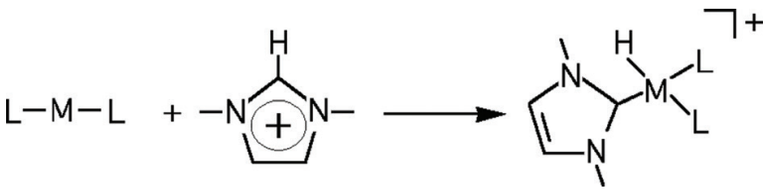

(M = Ni, Pd, Pt; L = 1, 3 - aryl-NHC, aryl = 2, 4, 6 - trimethylphenyl) (1)

http://dx.doi.org/10.5772/67567

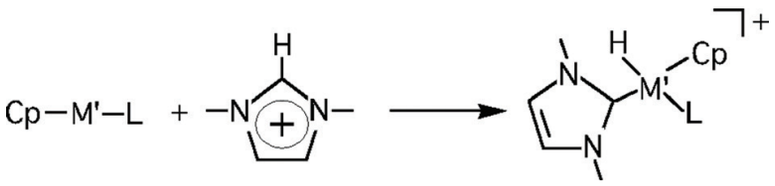

$$\left(M' = \text{Co, Rh, Ir; L} = \text{1, 3 - aryl - NHC, aryl} = \text{2, 4, 6 - trimethylphenyl}\right) \quad (2)$$

Since oxidative addition involves charge transfer from the metallic center of both L_2M and CpM′L to the approaching IC, an electron-donating L that increases the electron density on the central metal stabilizes its transition state and lowers the barrier height. That is to say, increasing the electron density on the central metal atom of both L_2M and CpM′L increases the chance of its triplet participating in the oxidative addition reaction (vide infra). Therefore, the reactivity of both substituted 14-electron L_2M and 16-electron CpM′L is verified by the singlet-triplet splitting ($\Delta E_{st} = E_{triplet} - E_{singlet}$), which can result from several factors, such as the effect of the geometrical structure (i.e., linear or bent for the L_2M system) [55], the nature of electron-withdrawal or electron-acceptance for the ancillary ligand, L, and the character of the central transition metal atom. In the organometallic field, the NHC groups are stronger σ-donors and weaker π-acceptor ligands than the traditional PR_3 ligands [47–50]. Therefore, the model systems (both L_2M and CpM′L complexes) that are studied in this work use the NHC as the ancillary ligand L.

Since the transition-metal-catalyzed reactions that contain imidazolium salt are both helpful and novel, a comprehensive understanding of the factors that control the magnitude of the activation barriers and the reaction enthalpies allows a greater understanding of their reactivity. Full realization of the factors that influence the reactivities of transition metal complexes with ICs benefits basic science and a continued expansion of their applications.

2. Theoretical methods

The geometries of all of the stationary points are fully optimized at the M06-L level of theory [57], using the Gaussian 09 program package [58]. These M06-2X calculations are executed using pseudo-relativistic effective core potentials on group 9 and group 10 elements, using the Def2-SVP basis sets [59–63]. These M06-L calculations are denoted as M06-L/Def2-SVP. Frequency computations are accomplished for all structures to verify that the reactants and products have no imaginary frequencies and that the transition states occupy only one imaginary frequency. The relative free energy (ΔG) at 298 K is computated at the M06-L/Def2-SVP level of theory.

3. The origin of the barrier and the reaction enthalpy for the oxidative addition of an imidazolium cation to transition metal complexes

In this section, the valence bond state correlation diagram (VBSCD) model [64–68] that was developed by Shaik and Pross is used to interpret the oxidative addition for an imidazolium cation to transition metal complexes. For the σ-bond insertion reaction, the system must have a number

of predetermined states, each of which is approximated by an appropriate electronic configuration [64–68]. In particular, there are two important configurations that contribute significantly to the total wave function, Ψ, and change the shape of the potential energy surface. **Figure 1** shows the qualitative behavior of the two configurations for the insertion of a transition-metal complex (L_nM) into a C(carbenic carbon)—H bond of an IC. The first line shows the reactant ground-state configuration, which connects the excited state for the products, denoted as the reactant configuration (I_R). The second line shows the excited configuration of the reactants, which connects the ground state of the products and is marked as the product configuration (I_P).

From the valence bond (VB) viewpoint, the reactions for the insertion of L_nM fragments into the C—H bond are illustrated in **1** and **2**, as shown in **Figure 1**. In the reactant configuration (I_R), which is labeled $^1[L_nM]^1[IC]$, the two electrons on the L_nM moiety are spin-paired to form a lone pair and the two electrons on the CH moiety are spin-paired to form a C—H σ bond. In the product configuration (I_P), which is labeled $^3[L_nM]^3[IC]$, the electron pairs are coupled to

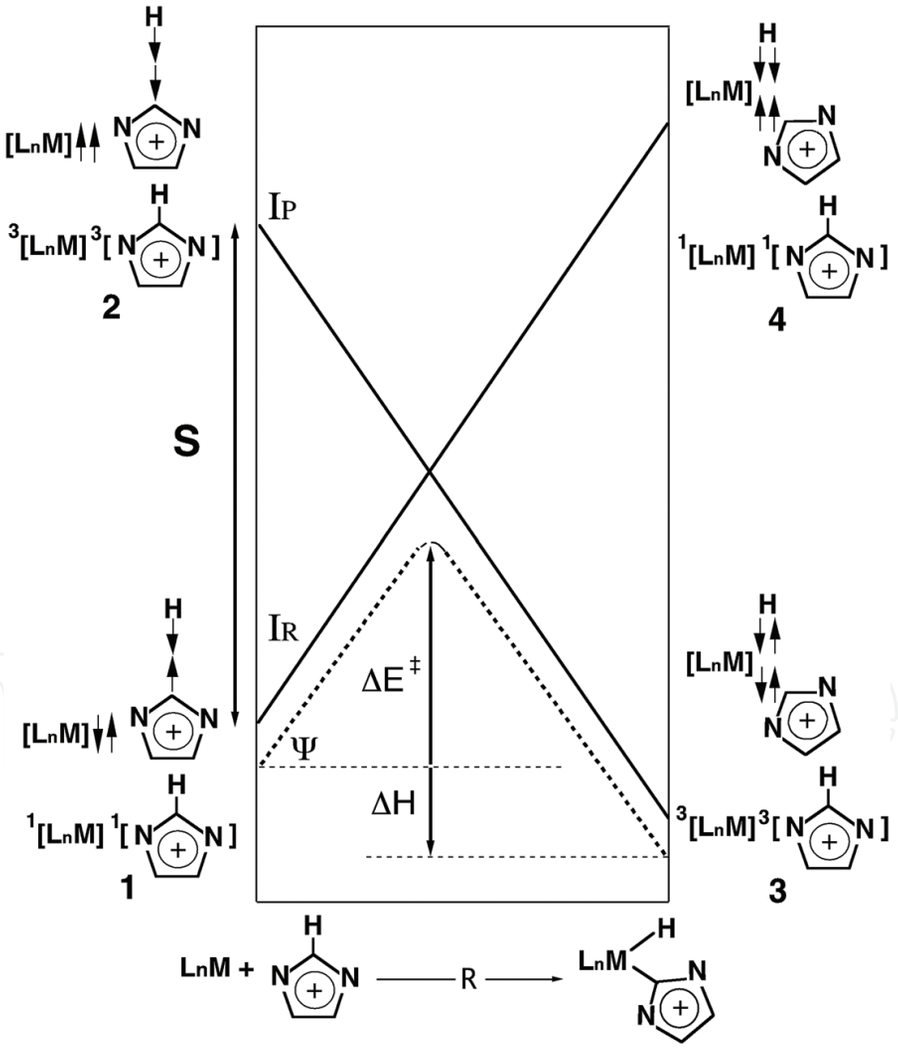

Figure 1. The energy diagram for an oxidative addition reaction, showing the formation of a state curve (Ψ) by mixing two configurations: the reactant configuration (I_R) and the product configuration (I_P). The reactants are separated by an energy gap, S. Configuration mixing near the crossing point causes an avoidance crossing (dotted line). For details see the text.

http://dx.doi.org/10.5772/67567

allow the formation of both an M—C and an M—H bond and the simultaneous breaking of a C—H bond. From the molecular orbital (MO) viewpoint, the representations of VB configurations **1** and **2** are respectively given in **3** and **4**.

It is proposed that the transition state for the reaction that inserts L_nM into a C—H bond is regarded as the respective triplet states of the reactants. It is worthy to note that these individual triplets are coupled to an overall singlet state. Since new M—C and M—H covalent bonds are formed in the product $L_nM(C)(H)$, the bond-prepared L_nM state must have at least two open shells. Therefore, the lowest state for this type is the triplet state. In other words, the bonding in the $L_nM(C)(H)$ product is between the triplet L_nM state and two doublet radicals (the C radical and the H radical). Similarly to the bonding in a water molecule, from the valence-bond point of view, it is represented as bonding between a triplet oxygen atom and two doublet hydrogen atoms [69].

As schematically illustrated in **Figure 1**, the singlet-triplet excitation energy plays a decisive role in the VBSCD model [64–68]. The singlet-triplet excitation energy (i.e., the energy between the I_R and the I_P) corresponds to the energy gap, S, in the VBSCD model. In terms of the reactants, I_R is the ground state and I_P is in an excited state whose energy is greater than I_R. When the reaction is in progress, the energy of I_R increases and that of I_P decreases. The transition state occurs at a point along the reaction coordinate where the energy curves for I_R and I_P cross (see the dotted curve in **Figure 1**). Finally, in terms of the products, I_R assumes the excited-state configuration and I_P a ground state. These two configurations cross. This is the simplest description of the ground state energy profiles for the chemical reactions of the related molecular systems [64–68].

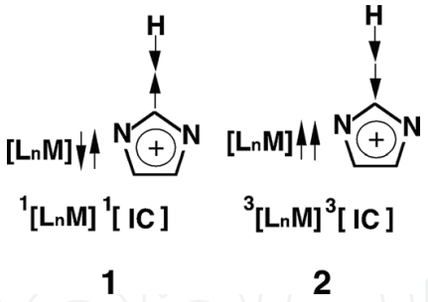

Scheme 2.

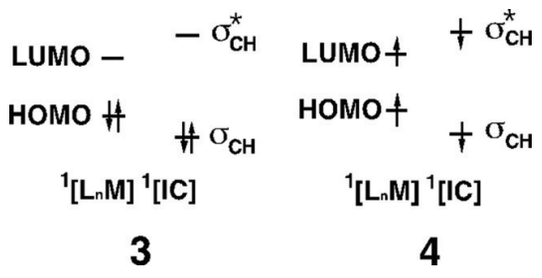

Scheme 3.

Figure 1 shows that the energy of point **2** (left in **Figure 1**), the anchor point for $^3[L_nM]^3[IC]$ in the reactant geometry, is governed by the singlet-triplet energy gap for both L_nM and C—H; i.e., ΔE_{st} (= $E_{triplet} - E_{singlet}$ for L_nM) + $\Delta E_{\sigma\sigma^*}$(= $E_{triplet} - E_{singlet}$ for C—H). In other words, the smaller the value of $\Delta E_{st} + \Delta E_{\sigma\sigma^*}$, the lower is the activation barrier and the more exothermic is the reaction [64–68]. If a reactant, L_nM, has a singlet ground state with a small triplet excitation energy, there is a greater probability that a triplet L_nM contributes to the singlet reaction and the reactions occur readily. Both the order of the singlet and triplet states and the magnitude of the singlet-triplet energy separation also determine the existence and the height of the energy barrier.

Since CH_2 and 16-electron CpML and 14-electron L_2M are isolobal [70], each has two valence orbitals with the same symmetry patterns (**5**), in which each fragment has one orbital of a′ and a″ symmetry.

In this qualitative theoretical treatment, the transition-metal fragment L_2M and CpML has an empty electrophilic orbital (i.e., a', as shown in **5**) that interacts with a filled hydrocarbon fragment orbital. This facilitates a concerted 1,2-hydrogen migration. In other words, the net molecular result of the insertion of the L_2M and CpML complexes into a C—H σ bond of an IC is that a new M—C σ bond and a new M—H σ bond are formed and the C—H σ bond of an IC is broken. This analysis is used to interpret the results in the following section.

4. Results and discussion

4.1. The geometries of the triscarbene-nickel-hydrido complex and the triscarbene-palladium-hydrido complex

The geometrical structures of the triscarbene-nickel-hydrido complex (**Pro-Ni**) and the triscarbene-palladium-hydrido complex (**Pro-Pd**) are firstly determined theoretically. The optimized geometries for these two species are computed at the M06-L/Def2-SVP level of theory. As

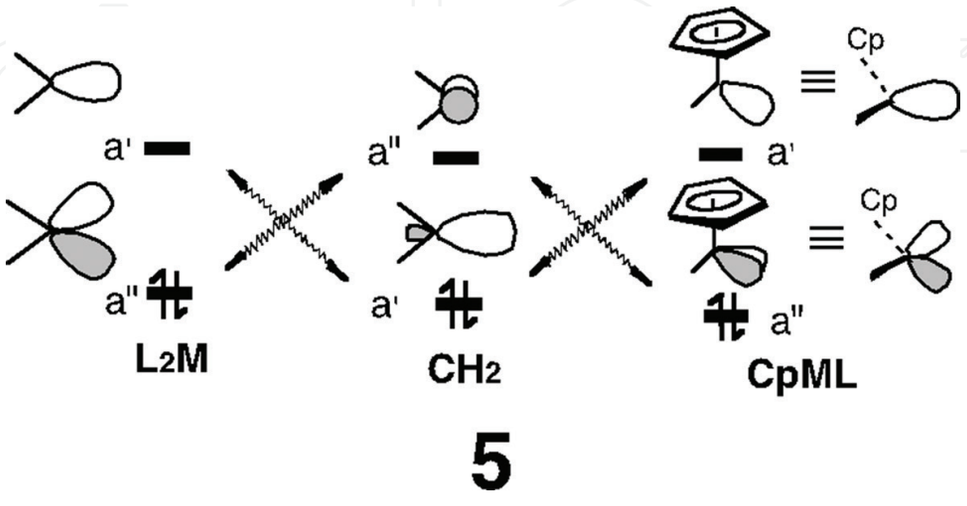

5

Scheme 4.

http://dx.doi.org/10.5772/67567

shown in **Figure 2**, the M06-L calculations show that the computed M—C bond lengths for both molecules (average 1.924 and 2.089 Å at M06-L) compare favorably with the average M—C bond lengths that are determined from X-ray data (1.907 and 2.057 Å) [43]. Similarly, the average values for the ∠C—M—C and ∠C—M—H angles for these two structures are calculated to be 98.26° and 82.58° (Ni) and 97.41° and 82.23° (Pd), which agrees reasonably well with the experimental data (97.85, 82.00, 95.94, and 84.00°, respectively) [43], as shown in **Figure 2**. Given the agreement between the M06-L method using the Def2-SVP basis set and the available experimental data [43], it is expected that the same relative accuracy is applicable to any discussion of their reactivities and the reaction mechanisms, for which experimental data are still not available.

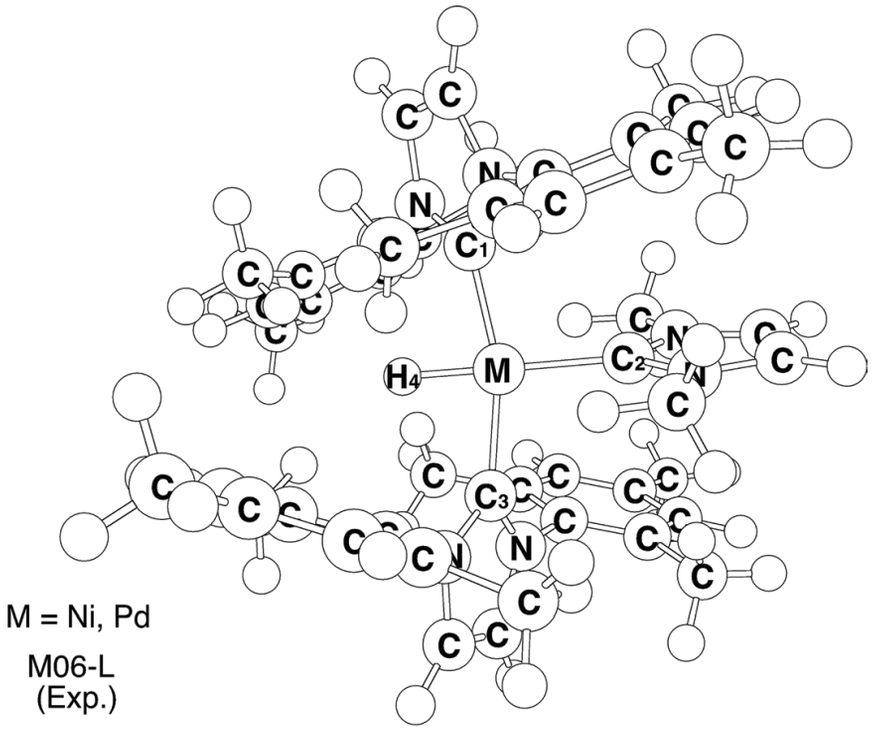

M	M-C_1	M-C_2	M-C_3	M-H_4	C_1-M-C_3
Ni	1.911	1.958	1.904	1.394	163.4
	(1.895)	(1.936)	(1.891)	(1.380)	(164.2)
	C_1-M-C_2	C_2-M-C_3	C_3-M-H_4	C_1-M-H_4	C_2-M-H_4
	98.29	98.24	83.76	81.39	179.0
	(97.30)	(98.40)	(83.00)	(81.00)	(179.0)
Pd	M-C_1	M-C_2	M-C_3	M-H_4	C_1-M-C_3
	2.057	2.144	2.067	1.572	167.2
	(2.031)	(2.111)	(2.030)	(1.570)	(168.0)
	C_1-M-C_2	C_2-M-C_3	C_3-M-H_4	C_1-M-H_4	C_2-M-H_4
	97.85	96.97	82.05	85.40	178.3
	(96.20)	(95.78)	(82.00)	(86.00)	(177.0)

Figure 2. Selected geometrical parameters (in Å and deg) for the triscarbene-nickel-hydrido complex (**Pro-Ni**) and the triscarbene-palladium-hydrido complex (**Pro-Pd**), calculated at the M06-L/Def2-SVP level of theory and a comparison with the experimental values [43]. Hydrogens are omitted for clarity.

4.2. The geometries and energetics of the L_2M + 1,2-dimethylimidazolium cation

The results for four regions on the potential energy surfaces for L_2M (M = Ni, Pd, Pt; L = 1,3-aryl-NHC, aryl = 2,4,6-trimethylphenyl) and 1,2-dimethylimidazolium cation (IC) are shown: 14-electron L_2M plus free IC (**Rea**), a precursor complex (**Pcx**), the transition state (**TS**), and the oxidative addition product (**Pro**). The fully optimized geometries for the key points, calculated at the M06-L/Def2-SVP level, are shown in **Figure 3**. The important geometrical parameters and relative energies and the potential energy profiles at the same level of theory are listed in **Table 1** and **Figure 4**, respectively. Four points are noteworthy.

1. For the optimized structures, see **Figure 3**. For the relative free energies, see **Figure 4**.

2. The C_3—H_4 bond distance in IC (reactant) is calculated to be 1.090 Å.

1. The reactants, **Rea-Ni, Rea-Pd**, and **Rea-Pt**, are computed as both low-spin (singlet) and high-spin (triplet state) complexes. The M06-L computations demonstrate that these transition metal complexes all adopt the singlet ground state. The computations also show that the singlet-triplet triplet free energy splitting (ΔE_{st}; kcal/mol) for these fragments are in the order: **Rea-Ni** (23.7) < **Rea-Pd** (50.1) < **Rea-Pt** (63.9). These values are much greater than those for other previously studied L_2M complexes that have various ancillary ligands [51–56]. Therefore, it is possible that the oxidative addition reactions (Eq. (1)) that are studied in this work proceed on the singlet surface. The singlet surface is therefore the focus of this study, from this point.

2. The optimized transition state structures (**TS-Ni, TS-Pd**, and **TS-Pt**) and arrows that indicate the main atomic motion in the transition state eigenvector are shown in **Figure 3**. These model computations show that the oxidative addition reactions that are studied using these model reactants all proceed in a concerted fashion via a three-center transition state, as shown in **Figure 3**, and all reactions are exothermic. It is noted that for the oxidative addition reactions involving the group 10 transition metals that are studied in this work, the free energies for the transition states are all less than those for the corresponding reactants. It is theoretically predicted that these oxidative addition reactions proceed readily, even at room temperature. Further supporting evidence comes from the fact that the oxidative additions between **Rea-Ni** and **Rea-Pd** species and an imidazolium cation have been experimentally proven to be easy [43].

3. According to the theoretical analysis of the VBSCD model that is discussed in Section 3, the smaller the value of ΔE_{st} for L_2M, the lower is the barrier height and the more exothermic is the reaction and the faster is the oxidative addition reaction. The model evidence confirms this prediction. For the M06-L calculations for the model systems that have group 10 transition metals, a plot of the activation barrier ($\Delta E^{\ddagger}$) versus the ΔE_{st} is shown, for which the best fit is $\Delta E^{\ddagger} = 0.518\Delta E_{st} - 11.2$. The linear correlation between ΔE_{st} and the Gibbs free energy (ΔG), which is also calculated at the same level of theory, is $\Delta G = 0.566\ \Delta E_{st} - 67.5$. The theoretical results definitely show that for the facile oxidative addition of C—H bonds, an understanding of the ΔE_{st} of the coordinatively unsaturated 14-electron L_2M is crucial, since it can be used to predict the reactivity of the reactants.

http://dx.doi.org/10.5772/67567

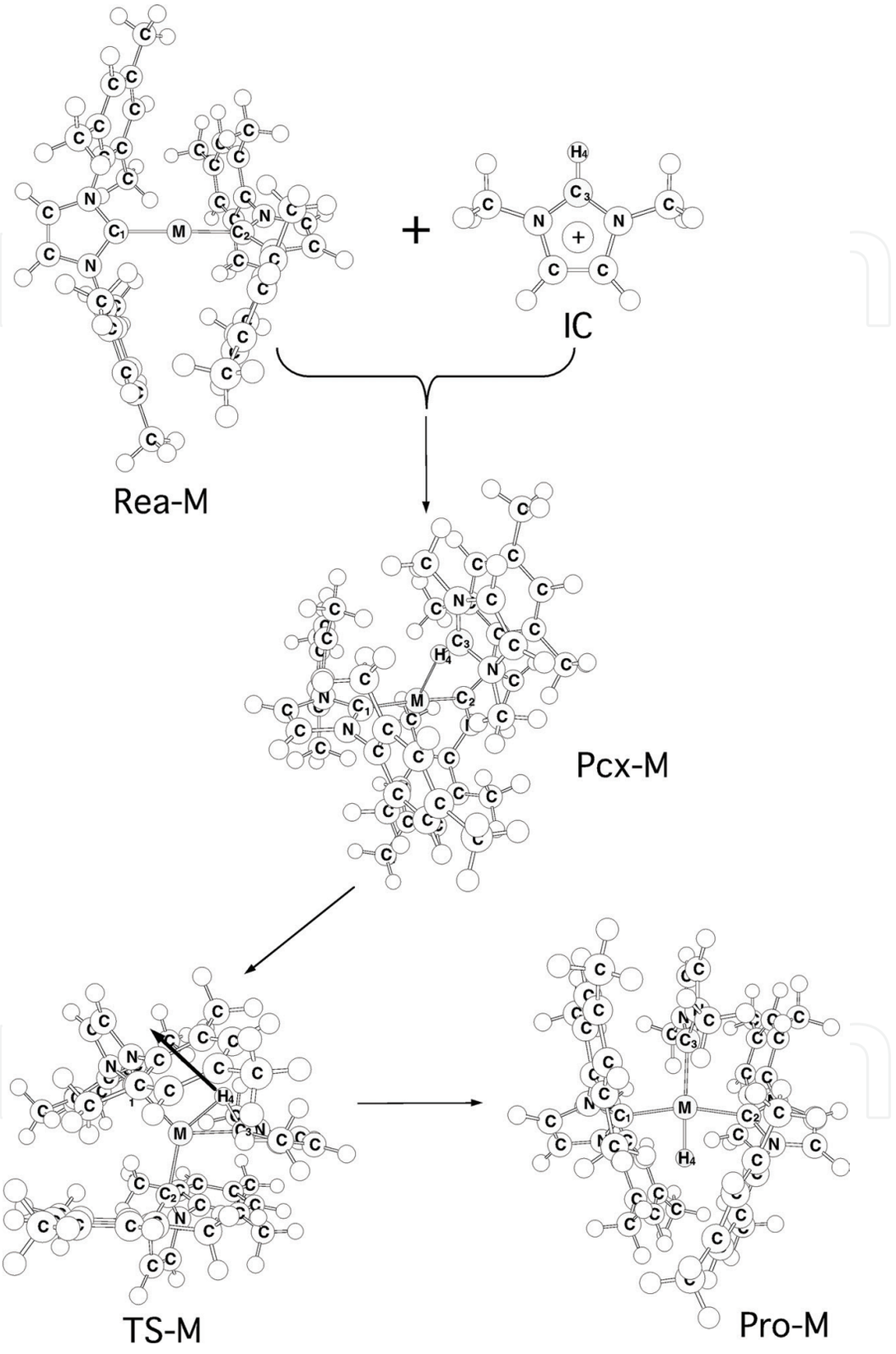

Figure 3. M06-L/Def2-SVP optimized geometries for the stationary points for the oxidative addition reactions of **Rea-M** (M = Ni, Pd, and Pt) molecules. For selected geometrical parameters and relative energies for each species, see **Table 1**. The bold arrows denote the main atomic motions in the transition state eigenvector. Some hydrogens are omitted for clarity.

	Geometrical structures					Energies	
Systems	**M-C_1**	**M-C_2**	**M-C_3**	**C_3-H_4**	**M-H_4**	**Δ*E***	**Δ*G***
Rea-Ni	1.836	1.836	–	–	–	0.0	0.0
Pcx-Ni	1.938	1.961	–	1.107	2.056	−50.24	−33.65
TS-Ni	1.981	1.947	1.886	1.482	1.527	−49.38	−32.26
Pro-Ni	1.911	1.904	–	1.985	1.394	−69.31	−54.36
Rea-Pd	2.015	2.015	–	–	–	0.0	0.0
Pcx-Pd	2.050	2.053	–	1.115	2.105	−39.69	−23.67
TS-Pd	2.159	2.138	2.039	1.437	1.679	−25.99	−8.417
Pro-Pd	2.057	2.067	–	2.144	1.572	−55.36	−38.23
Rea-Pt	2.003	2.003	–	–	–	0.0	0.0
Pcx-Pt	2.022	2.019	–	1.119	2.134	−41.35	−22.46
TS-Pt	2.128	2.064	2.067	1.333	1.797	−16.49	−1.384
Pro-Pt	2.054	2.060	–	2.139	1.621	−47.52	−31.98

Table 1. Selected geometrical parameters (bond distances in Å), relative energies Δ*E* (zero-point corrected; kcal mol^{-1}) and relative Gibbs free energies Δ*G* (kcal mol^{-1}) at 298 K at the M06-L/Def2-SCP level of theory for the optimized stationary points on the oxidative addition reactions (Eq. (1)) [1–30].

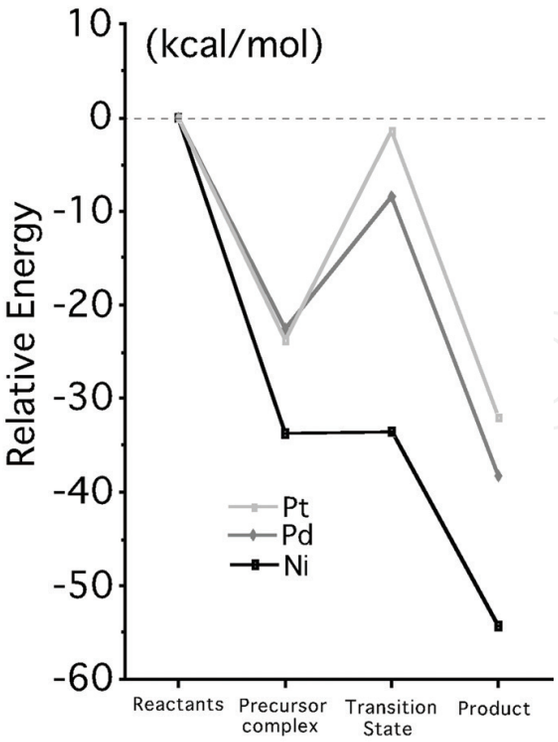

Figure 4. The reaction energy profile (in kcal/mol) for the oxidative addition reactions: L_2M + 1,2-dimethylimidazolium cation (M = Ni, Pd, and Pt; L = 1,3-aryl-NHC, aryl = 2,4,6-trimethylphenyl). All of the energies are calculated at the M06-L/Def2-SVP level. See also **Table 1** and **Figure 3**.

http://dx.doi.org/10.5772/67567

4.3. The geometries and energetics of the CpM′+ 1,2-dimethylimidazolium cation

Similarly to the study of the L_2M system, the M06-L/Def2-SVP level is also used to study the mechanisms for the oxidative addition reactions for CpM′L (M′ = Co, Rh, Ir; L = 1,3-aryl-NHC, aryl = 2,4,6-trimethylphenyl), as shown in **Figure 5**. The relative M06-L energies and the key geometrical parameters for the stationary points are also listed in **Table 2**. The corresponding potential energy profiles are given in **Figure 6**. Three interesting conclusions can be drawn from these figures and the table.

1. For the optimized structures, see **Figure 5**. For the relative free energies, see **Figure 6**.

2. The C_2—H_3 bond distance in IC (reactant) is calculated to be 1.090 Å.

1. The M06-L calculations in **Table 2** show that the ground states for the CpCoL and CpIrL fragments are triplets, but the CpRhL complex is a singlet. The M06-L results also show that the ΔE_{st} value for the CpCoR and CpIrR fragments are respectively computed to be− 8.3 and − 0.88 kcal/mol and the ΔE_{st} of CpRhR was predicted to be 10.2 kcal/mol. It is worthy to note that whenever a reactant contains a heavy atom that is not necessarily directly included in the reaction, a strong spin-orbit coupling (SOC) can occur [71–75]. That is, because of the presence of the heavy atom, a triplet reactant can cause a spin-inversion process. It transfers to the singlet reactant and then forces the singlet reaction. Since these theoretical calculations show that both the CpCoR and the CpIrR species have a small value for ΔE_{st} and a heavier transition metal is involved, the SOC is expected to be substantial for the oxidative additions and these would eventually proceed in the singlet chemical reactions.

2. **Figure 6** shows that, similar to the case for L_2M molecules, the energy of the transition state for Co, Rh, and Ir is less than that for the reactants, which demonstrates that the CpM′L (M′ = Co, Rh, and Ir) complexes readily overcome the energy barrier and then undergo oxidative addition into the C—H bond of IC in a concerted fashion, even at room temperature. The model computations show that the oxidative addition of a CpM′L fragment that has a group 9 metal (M′) decreases in the order: CpCoL > CpIrL > CpRhL. For the reverse process (right to left in **Figure 6**), the barriers to reductive elimination for the Co, Rh, and Ir systems have much higher energies than those for the corresponding oxidative addition. The theoretical evidence demonstrates that these CpM′L complexes undergo oxidative additions more easily than reductive eliminations, as noted in the introduction. That is to say, because the attached NHC groups readily donate electrons, the electrons in the metal, M′, are abundant and the CpM′L readily allows oxidative additions with the incoming molecules. The theoretical studies suggest that the CpM′L molecules prefer to undergo oxidative addition reactions with the imidazolium cation, even at room temperature.

3. According to the VBSCD model, the smaller the ΔE_{st} value for CpM′L (if $\Delta E_{\sigma\sigma^*}$ is a constant), the lower is the barrier height, the more exothermic is the reaction and the faster is the oxidative addition reaction [64–68]. The M06-L/Def2-SVP results support this prediction. The M06-L calculations show that value for ΔE_{st} (kcal/mol) increases in the order: CpCoL (−8.3) < CpIrL (−0.77) < CpRhL (+8.0). As shown in **Table 2**, both the

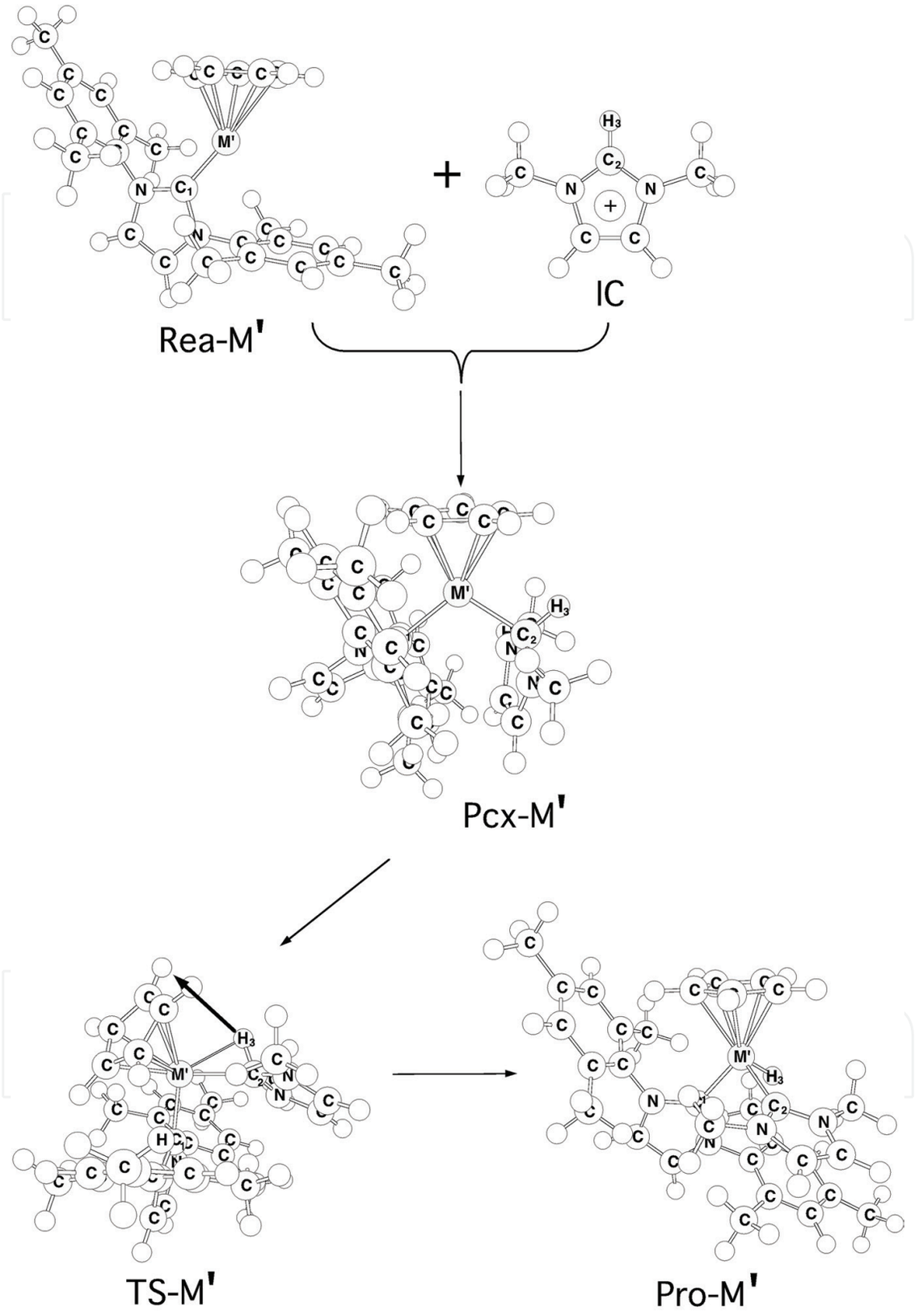

Figure 5. M06-L/Def2-SVP optimized geometries for the stationary points for the oxidative addition reactions of **Rea-M′** (M′ = Co, Rh, and Ir) molecules. For the selected geometrical parameters and relative energies for each species, see **Table 2**. The bold arrows denote the main atomic motions in the transition state eigenvector. Some hydrogens are omitted for clarity.

http://dx.doi.org/10.5772/67567

	Geometrical structures				Energies	
Systems	**M′-C_1**	**M′-C_2**	**C_2-H_3**	**M′-H_3**	**Δ*E***	**Δ*G***
Rea-Co	1.858	–	–	–	0.0	0.0
Pcx-Co	1.981	1.964	1.101	2.569	−20.16	−8.462
TS-Co	1.967	2.044	1.130	2.043	−17.45	+0.542
Pro-Co	1.947	1.920	2.337	1.472	−79.40	−62.38
Rea-Rh	1.953	–	–	–	0.0	0.0
Pcx-Rh	2.055	2.080	1.101	2.634	−31.35	−17.19
TS-Rh	2.075	2.158	1.147	2.002	−22.41	−6.193
Pro-Rh	2.046	2.017	2.411	1.569	−55.43	−39.08
Rea-Ir	1.923	–	–	–	0.0	0.0
Pcx-Ir	2.055	2.084	1.104	2.665	−39.30	−21.79
TS-Ir	2.037	2.147	1.146	2.156	−28.16	−10.98
Pro-Ir	2.043	2.029	2.448	1.594	−59.43	−46.20

Table 2. Key geometrical parameters (bond distances in Å), relative energies Δ*E* (zero-point corrected; kcal mol^{-1}) and relative Gibbs free energies Δ*G* (kcal mol^{-1}) at 298 K, calculated at the M06-L/Def2-SCP level of theory, for the optimized stationary points on the oxidative addition reactions (Eq. (2)) [1–30].

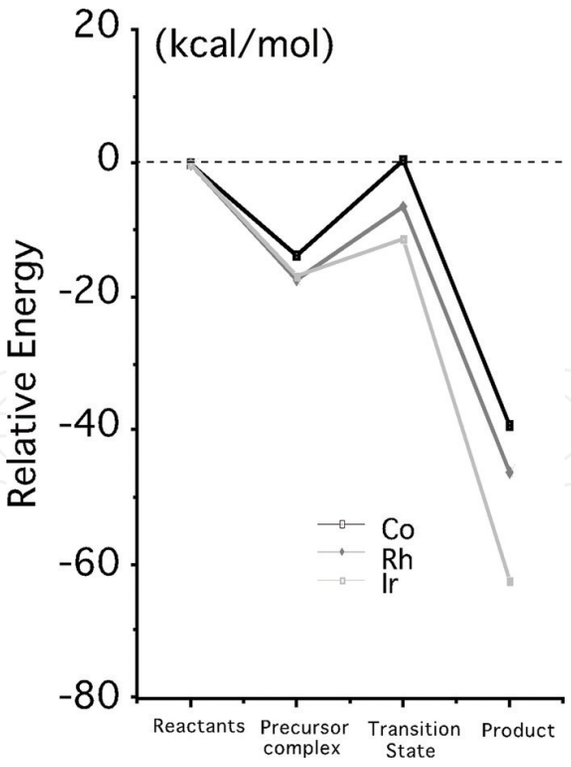

Figure 6. The reaction energy profile (in kcal/mol) for the oxidative addition reactions: CpML + 1,2-dimethylimidazolium cation (M = Co, Rh, and Ir; L = 1,3-aryl-NHC, aryl = 2,4,6-trimethylphenyl). All of the energies are calculated at the M06-L/Def2-SVP level. See also **Table 1** and **Figure 3**.

activation energies ($\Delta E^{\ddagger}$) and the Gibbs free energies (ΔG) follow the same order as the ΔE_{st} value (kcal/mol): Co (+9.28, −62.4) < Ir (+10.8, −46.2 kcal/mol) < Rh (+11.0, −39.1). In order to determine a good model for the facile oxidative addition of 16-electron CpM′L to a C-H bond of an imidazolium cation, an understanding of the ΔE_{st} of the coordinatively unsaturated CpM′L is important.

5. Conclusions

In summary, the theoretical evidence demonstrates that both a 14-electron L_2M complex and a 16-electron CpM′Lcomplex with a better electron-donating ligand, L (such as NHC), result in a smaller value for ΔE_{st} and allow a more facile oxidative addition to the saturated C—H bond. This theoretical study also demonstrates that, in terms of the VBSCD model, the ΔE_{st} value is a useful foundation for predicting the relative magnitude of the activation barriers and the reaction enthalpies for the activation of an imidazolium cation by L_2M and CpM′L. Although the computed magnitude of the barrier and the predicted geometry for the transition state for these reactions are dependent on the level of theory that is used, these qualitative predictions are in good agreement with the theoretical results that are presented here and with the available experimental observations.

It is hoped that this study will stimulate for further research into the subject.

Acknowledgements

The authors are grateful to the National Center for High-Performance Computing of Taiwan for generous amounts of computing time and the Ministry of Science and Technology of Taiwan for the financial support.

Author details

Hsin-Yi Liao[1]*, Jia-Syun Lu[2] and Ming-Der Su[2,3]*

*Address all correspondence to: midesu@mail.ncyu.edu.tw and hyliao@tea.ntue.edu.tw

1 Department of Science Education, National Taipei University of Education, Taipei, Taiwan

2 Department of Applied Chemistry, National Chiayi University, Chiayi, Taiwan

3 Department of Medicinal and Applied Chemistry, Kaohsiung Medical University, Kaohsiung, Taiwan

http://dx.doi.org/10.5772/67567

References

[1] Herrmann WA, Köcher C. N-Heterocyclic carbenes. Angewandte Chemie International Edition in English. 1997;**36**:2162-2187

[2] McGuinness DS, Green MJ, Cavell KJ, Skelton BW, White AH. Synthesis and reaction chemistry of mixed ligand methylpalladium–carbene complexes. Journal of Organometallic Chemistry. 1998;**565**:165-178

[3] McGuinness DS, Cavell KJ, Skelton BW, White AH. Zerovalent palladium and nickel complexes of heterocyclic carbenes: Oxidative addition of organic halides, carbon-carbon coupling processes, and the Heck reaction. Organometallics. 1999;**18**:1596-1605

[4] Carmichael AJ, Earle MJ, Holbrey JD, McCormac PB, Seddon KR. The Heck reaction in ionic liquids: A multiphasic catalyst system. Organic Letters. 1999;**1**:997-1000

[5] McGuinness DS, Cavell KJ. Donor-functionalized heterocyclic carbene complexes of palladium (ii): Efficient catalyst C—C coupling reaction. Organometallics. 2000;**19**:741-748

[6] Xu L, Chen W, Xiao J. Heck reaction in ionic liquids and the in situ identification of N-heterocyclic carbene complexes of palladium. Organometallics. 2000;**19**:1123

[7] McGuinness DS, Cavell KJ. Reaction of CO with a methylpalladium heterocyclic carbene complex: Product decomposition routes—Implications for catalytic carbonylation processes. Organometallics. 2000;**19**:4918

[8] Mathews CJ, Smith PJ, Welton T. Palladium catalysed Suzuki cross-coupling reactions in ambient temperature ionic liquids. Chemical Communications. 2000;**14**:1249-1250

[9] McGuinness DS, Saendig N, Yates BF, Cavell KJ. Kinetic and density functional studies on alkyl-carbene elimination from PdII heterocyclic carbene complexes: A new type of reductive elimination with clear implications for catalysis. Journal of the American Chemical Society. 2001;**123**:4029-4040

[10] McGuinness DS, Cavell KJ, Yates BF, Skelton BW, White AH. Oxidative addition of the imidazolium cation to zerovalent Ni, Pd, and Pt: A combined density functional and experimental study. Journal of the American Chemical Society. 2001;**123**:8317-8328

[11] Duin MA, Clement ND, Cavell KJ, Elsevier CJ. C–H activation of imidazolium salts by Pt(0) at ambient temperature: Synthesis of hydrido platinum bis(carbene) compounds. Journal of Chemical Communication. 2003;**3**:400-401

[12] Dubinina GG, Furutachi H, Vicic DA. Active trifluoromethylating agents from well-defined copper(I)-CF_3 complexes. Journal of the American Chemical Society. 2008;**130**8600-8601

[13] Boydston AJ, Xia Y, Kornfield JA, Gorodetskaya IA, Grubbs RH. Cyclic ruthenium-alkylidene catalysts for ring-expansion metathesis polymerization. Journal of the American Chemical Society. 2008;**130**:12775-12782

[14] Liu Q, Perreault S, Rovis T. Catalytic asymmetric intermolecular stetter reaction of glyoxamides with alkylidenemalonates. Journal of the American Chemical Society. 2008;**130**:14066-14067

[15] Park EJ, Kim SH, Chang S. Copper-catalyzed reaction of α-aryldiazoesters with terminal alkynes: A formal [3+2] cycloaddition route leading to indene derivatives. Journal of the American Chemical Society. 2008;**130**:17268-17269

[16] Nordstrøm LU, Vogt H, Madsen R. Amide synthesis from alcohols and amines by the extrusion of dihydrogen. Journal of the American Chemical Society. 2008;**130**:17672-17673

[17] Marion N, Ramón RS, Nolan SP. [(NHC)Au^{I}]-catalyzed acid-free alkyne hydration at part-per-million catalyst loadings. Journal of the American Chemical Society. 2009;**131**: 448-449

[18] Horino Y, Yamamoto T, Ueda K, Kuroda S, Toste D. Au(I)-catalyzed cycloisomerizations terminated by sp^3 C—H bond insertion. Journal of the American Chemical Society. 2009;**131**:2809-2811

[19] Lee Y, Hoveyda H. Efficient boron-copper additions to aryl-substituted alkenes promoted by NHC-based catalysts. Enantioselective Cu-catalyzed hydroboration reactions. Journal of the American Chemical Society. 2009;**131**:3160-3161

[20] Raynaud J, Absalon C, Gnanou Y, Taton D. N-Heterocyclic carbene-induced zwitterionic ring-opening polymerization of ethylene oxide and direct synthesis of α,ω-difunctionalized poly(ethylene oxide)s and poly(ethylene oxide)-b-poly(ε-caprolactone) block copolymers. Journal of the American Chemical Society. 2009;**131**:3201-3209

[21] Jana A, Schulzke C, Roesky HW. Oxidative addition of ammonia at a silicon(II) center and an unprecedented hydrogenation reaction of compounds with low-valent group 14 elements using ammonia borane. Journal of the American Chemical Society. 2009;**131**:4600-4601

[22] Häller LJL, Page MJ, Macgregor SA, Mahon MF, Whittlesey MK. Activation of an alkyl C—H bond geminal to an agostic interaction: An unusual mode of base-induced C—H activation. Journal of the American Chemical Society. 2009;**131**:4604-4605

[23] Jeong W, Shin EJ, Culkin DA, Hedrick JL, Waymouth RM. Zwitterionic polymerization: A kinetic strategy for the controlled synthesis of cyclic polylactide. Journal of the American Chemical Society. 2009;**131**:4884-4891

[24] Boydston AJ, Holcombe TW, Unruh DA, Fréchet MJ, Grubbs RH. A direct route to cyclic organic nanostructures via ring-expansion metathesis polymerization of a dendronized macromonomer. Journal of the American Chemical Society. 2009;**131**:5388-5389

[25] Aktas H, Slootweg JC, Schakel M, Ehlers AW, Lutz M, Spek AL, Lammertsma K. N-Heterocyclic carbene-functionalized ruthenium phosphinidenes: What a difference a twist makes. Journal of the American Chemical Society. 2009;**131**:6666-6667

[26] Iwai T, Fujihara T, Terao J, Tsuji Y. Iridium-catalyzed addition of acid chlorides to terminal alkynes. Journal of the American Chemical Society. 2009;**131**:6668-6669

[27] Galan BR, Pitak M, Gembicky M, Keister JB, Diver ST. Ligand-promoted carbene insertion into the aryl substituent of an n-heterocyclic carbene ligand in ruthenium-based metathesis catalysts. Journal of the American Chemical Society. 2009;**131**:6822-6832

[28] Xiong Y, Yao S, Driess M. An isolable NHC-supported silanone. Journal of the American Chemical Society. 2009;**131**:7562-7563

[29] Zeng X, Frey GD, Kinjo R, Donnadieu B, Bertrand G. Synthesis of a simplified version of stable bulky and rigid cyclic (alkyl)(amino)carbenes, and catalytic activity of the ensuing gold(I) complex in the three-component preparation of 1,2-dihydroquinoline derivatives. Journal of the American Chemical Society. 2009;**131**:8690-8696

[30] Chiang P-C, Rommel M, Bode JW. α'-Hydroxyenones as mechanistic probes and scope-expanding surrogates for α,β-unsaturated aldehydes in N-heterocyclic carbene-catalyzed reactions. Journal of the American Chemical Society. 2009;**131**:8714-8718

[31] Herrmann WA, Elison M, Fischer J, Kocher C, Artus GRJ. Metal complexes of N-heterocyclic carbenes—A new structural principle for catalysts in homogeneous catalysis. Angewandte Chemie International Edition in English. 1995;**34**:2371-2374

[32] Herrmann WA, Runte O, Artus G. Synthesis and structure of an ionic beryllium-"carbene" complex. Journal of Organometallic Chemistry. 1995;**501**:C1–C4

[33] Herrmann WA, Goossen LJ, Köcher C, Artus GRJ. Chiral heterocylic carbenes in asymmetric homogeneous catalysis. Angewandte Chemie International Edition in English. 1996;**35**:2805-2807

[34] Herrmann WA, Elison M, Fischer J, Köcher C, Artus GRJ. N-Heterocyclic carbened$^{[+]}$: Generation under mild conditions and formation of group 8-10 transition metal complexes relevant to catalysis. Chemistry: A European Journal. 1996;**2**:772-780

[35] Welton T. Room-temperature ionic liquids. solvents for synthesis and catalysis. Chemical Reviews. 1999;**99**:2071-2084

[36] Wasserscheid P, Keim W. Ionische flüssigkeiten—neue lösungen für die übergangsmetallkatalyse. Angewandte Chemie. 2000;**112**:3926-3945

[37] Wasserscheid P, Keim W. Ionic liquids—new "solutions" for transition metal catalysis. Angewandte Chemie International Edition. 2000;**39**:3772-3789

[38] Sheldon R. Catalytic reactions in ionic liquids. Chemical Communications. 2001;**23**: 2399-2407

[39] Dupont J, Souza RF, Suarez PAZ. Ionic liquid (molten salt) phase organometallic catalysis. Chemical Reviews. 2002;**102**:3667-3692

[40] Mathews CJ, Smith PJ, Welton T, White AJP, Williams DJ. In situ formation of mixed phosphine-imidazolylidene palladium complexes in room-temperature ionic liquids. Organometallics. 2001;**20**:3848-3850

[41] Dullius JEL, Suarez PAZ, Einloft S, Souza RF, Dupont J, Fischer J, Cian AD. Selective catalytic hydrodimerization of 1,3-butadiene by palladium compounds dissolved in ionic liquids. Organometallics. 1998;**17**:815-819

[42] Fonseca GS, Umpierre AP, Fichtner PFP, Teixeira SR, Dupont J. The use of imidazolium ionic liquids for the formation and stabilization of Ir^0 and Rh^0 nanoparticles: Efficient catalysts for the hydrogenation of arenes. Chemistry: A European Journal. **2003;9**:3263-3269

[43] Clement ND, Cavell KJ, Jones C, Elsevier CJ. Oxidative addition of imidazolium salts to Ni^0 and Pd^0: Synthesis and structural characterization of unusually stable metal–hydride complexes. Angewandte Chemie International Edition. 2004;**43**:1277-1279

[44] Arduengo AJIII, Harlow RL, Kline M. A stable crystalline carbine. Journal of the American Chemical Society. 1991;**113**:361-363

[45] Arduengo AJIII, Dias HVR, Harlow RL, Kline M. Electronic stabilization of nucleophilic carbenes. Journal of the American Chemical Society. 1992;**114**:5530-5534

[46] Arduengo AJIII. Looking for stable carbenes: The difficulty in starting anew. Accounts of Chemical Research. 1999;**32**:913-921

[47] Regitz M. Stable carbenes—illusion or reality? Angewandte Chemie International Edition in English. 1991;**30**:674-676

[48] Enders D, Balensiefer T. Nucleophilic carbenes in asymmetric organocatalysis. Accounts of Chemical Research. 2004;**37**:534-541

[49] Johnson JS. Catalyzed reactions of acyl anion equivalents. Angewandte Chemie International Edition. 2004;**43**:1326-1328

[50] Nair V, Bindu S, Sreekumar V. N-Heterocyclic carbenes: reagents, not just ligands!. Angewandte Chemie International Edition. 2004;**43**:5130-5135

[51] Hackett M, Ibers JA, Jernakoff P, Whitesides GM. cis-[Bis(dicyclohexylphosphino)ethane] platinum(0) reacts with unactivated carbon-hydrogen bonds. Journal of the American Chemical Society. 1986;**108**:8094-8095

[52] Hackett M, Ibers JA, Whitesides GM. Activation of the carbon-hydrogen bonds of benzene by reaction with [bis(dicyclohexylphosphino)ethane]platinum(0), generated by the thermolysis of cis-[bis(dicyclohexylphosphino)ethane]hydridoneopentylplatinum(II). Journal of the American Chemical Society . 1988;**110**:1436-1448

[53] Hackett M, Whitesides GM. [Bis(dicyclohexylphosphino)ethane]platinum(0). Reactions with alkyl, (trimethylsilyl)methyl, aryl, benzyl, and alkynyl carbon-hydrogen bonds. Journal of the American Chemical Society. 1988;**110**:1449-1462

[54] Sakaki S, Biswas B, Sugimoto M. Computational evidence for a free silylium ion. Organometallics. 1998;**17**:278-280

[55] Su M-D, Chu S-Y. Theoretical study of oxidative addition and reductive elimination of 14-electron d^{10} ML_2 complexes: a $ML_2 + CH_4$ (M = Pd, Pt; L = CO, PH_3, $L_2 = PH'_2CH_2CH_2PH_2$) case study. Inorganic Chemistry. 1998;**37**:3400-3406

[56] Sakaki S, Kai S, Sugimoto M. Theoretical study on σ-bond activation of $(HO)_2B–XH_3$ by $M(PH_3)_2$ (X = C, Si, Ge, or Sn; M = Pd or Pt). Noteworthy contribution of the boryl p_π orbital to M-boryl bonding and activation of the B–X σ-bond. Organometallics. 1999;**18**:4825-4837

[57] Zhao Y, Truhlar DG. Density functionals with broad applicability in chemistry. Accounts of Chemical Research. 2008;**41**:157-167

[58] Frisch MJ, Trucks GW, Schlegel HB, Scuseria GE, Robb MA, Cheeseman JR, Scalmani G, Barone V, Mennucci B, Petersson GA, Nakatsuji H, Caricato M, Li X, Hratchian HP, Izmaylov AF, Bloino J, Zheng G, Sonnenberg JL, Hada M, Ehara M, Toyota K, Fukuda R, Hasegawa J, Ishida M, Nakajima T, Honda Y, Kitao O, Nakai H, Vreven T, Montgomery Jr JA, Peralta JE, Ogliaro F, Bearpark M, Heyd JJ, Brothers E, Kudin KN, Staroverov VN, Keith T, Kobayashi R, Normand J, Raghavachari K, Rendell A, Burant JC, Iyengar SS, Tomasi J, Cossi M, Rega N, Millam JM, Klene M, Knox JE, Cross JB, Bakken V, Adamo C, Jaramillo J, Gomperts R, Stratmann RE, Yazyev O, Austin A J, Cammi R, Pomelli C, Ochterski JW, Martin RL, Morokuma K, Zakrzewski VG, Voth GA, Salvador P, Dannenberg JJ, Dapprich S, Daniels AD, Farkas O, Foresman JB, Ortiz JV, Cioslowski J, Fox DJ. Wallingford, CT: Gaussian, Inc.; 2013

[59] Andrae D, Haeussermann U, Dolg M, Stoll H, Preuss H. Energy-adjusted ab initio pseudopotentials for the second and third row transition elements. Theoretica Chimica Acta. 1990;**77**:123-141

[60] Metz B, Stoll H, Dolg M. Small-core multiconfiguration-Dirac–Hartree–Fock-adjusted pseudopotentials for post-d main group elements: Application to PbH and PbO. Journal of Chemical Physics, 2000;**113**:2563-2569

[61] Peterson KA, Figgen D, Goll E, Stoll H, Dolg M. Systematically convergent basis sets with relativistic pseudopotentials. II. Small-core pseudopotentials and correlation consistent basis sets for the post-*d* group 16-18 elements. Journal of Chemical Physics. 2003;**119**:11113-11123

[62] Leininger T, Nicklass A, Kuechle W, Stoll H, Dolg M, Bergner A. The accuracy of the pseudopotential approximation: Non-frozen-core effects for spectroscopic constants of alkali fluorides XF (X = K, Rb, Cs). Chemical Physics Letters. 1996;**255**:274-280

[63] Kaupp M, Schleyer PV, Stoll H, Preuss HJ. Pseudopotential approaches to Ca, Sr, and Ba hydrides. Why are some alkaline earth MX2 compounds bent? Chemical Physics. 1991;**94**:1360-1366

[64] Shaik S, Schlegel HB, Wolfe S. Theoretical Aspects of Physical Organic Chemistry. USA: John Wiley & Sons Inc; 1992

[65] Pross A. Theoretical and Physical Principles of Organic Reactivity. USA: John Wiley & Sons Inc; 1995

[66] Shaik S, Hiberty PC. A Chemist's Guide to Valence Bond Theory. USA: Wiley; 2008

[67] Shaik, S. What happens to molecules as they react? A valence bond approach to reactivity. Journal of the American Chemical Society. 1981;**103**:3692-3701

[68] Shaik S, Shurki A. Valence bond diagrams and chemical reactivity. Angewandte Chemie International Edition. 1999;**38**:586-625

[69] Siegbahn PEM. Comparison of the C—H activation of methane by M(C5H5)(CO) for M = cobalt, rhodium, and iridium. Journal of the American Chemical Society. 1996;**118**:1487-1496

[70] Hoffmann R. Building bridges between inorganic and organic chemistry (Nobel lecture). Angewandte Chemie International Edition in English. 1982;**21**:711-724

[71] Su M-D. Mechanism for di-π-methane rearrangements in nonconjugated systems. Chemical Physics Letters. 1995;**237**:317-322

[72] Su M-D. Mechanism for the photorearrangements of cyclohexadienes. Journal of Organic Chemistry 1995;**60**:6621-6623

[73] Su M-D. Role of spin-orbit coupling and symmetry in triplet carbenic addition chemistry. Journal of Physical Chemistry. 1996;**100**:4339-4349

[74] Su M-D. The role of spin-orbit coupling and symmetry in photochemical rearrangements of α,β-unsaturated cyclic ketones. Chemical Physics. 1996;**205**:277-308

[75] Su M-D. The role of spin-orbit coupling and symmetry in oxadi-π-methane rearrangements and some related photochemical reactions. Journal of Organic Chemistry 1996;**61**: 3080-3087